ACS APPLIED MATERIALS & INTERFACES

Research Article

Cite This: ACS Appl. Mater. Interfaces 2019, 11, 14997−15006

www.acsami.org

Flexible, Tunable, and Ultrasensitive Capacitive Pressure Sensor with Microconformal Graphene Electrodes

Jun Yang,[†,‡] Shi Luo,[†] Xi Zhou,[†] Jialu Li,[†] Jianting Fu,[†] Weidong Yang,[*,§] and Dapeng Wei[*,†]

[†]Chongqing Key Laboratory of Multi-Scale Manufacturing Technology, Chongqing Institute of Green and Intelligent Technology, Chinese Academy of Sciences, Chongqing 400714, P. R. China

[‡]University of Chinese Academy of Sciences, Beijing 100049, P. R. China

[§]Department of Materials Science and Engineering, National University of Singapore, Singapore 117576, Singapore

Supporting Information

ABSTRACT: High-performance flexible pressure sensors are highly desirable in health monitoring, robotic tactile, and artificial intelligence. Construction of microstructures in dielectrics and electrodes is the dominating approach to improving the performance of capacitive pressure sensors. Herein, we have demonstrated a novel three-dimensional microconformal graphene electrode for ultrasensitive and tunable flexible capacitive pressure sensors. Because the fabrication process is controllable, the morphologies of the graphene that is perfectly conformal with the electrode are controllable consequently. Multiscale morphologies ranging from a few nanometers to hundreds of nanometers, even to tens of micrometers, have been systematically investigated, and the high-performance capacitive pressure sensor with high sensitivity (3.19 kPa^{-1}), fast response (30 ms), ultralow detection limit (1 mg), tunable-sensitivity, high flexibility, and high stability was obtained. Furthermore, an ultrasensitivity of 7.68 kPa^{-1} was successfully achieved via symmetric double microconformal graphene electrodes. The finite element analysis indicates that the microstructured graphene electrode can enhance large deformation and thus effectively improve the sensitivity. Additionally, the proposed pressure sensors are demonstrated with practical applications including insect crawling detection, wearable health monitoring, and force feedback of robot tactile sensing with a sensor array. The microconformal graphene may provide a new approach to fabricating controllable microstructured electrodes to enhance the performance of capacitive pressure sensors and has great potential for innovative applications in wearable health-monitoring devices, robot tactile systems, and human−machine interface systems.

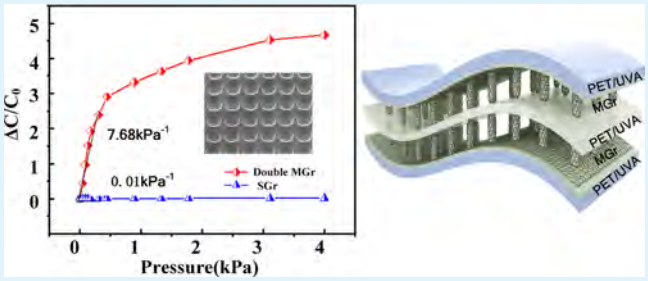

KEYWORDS: *capacitive pressure sensor, microconformal graphene electrodes, ultrasensitive, flexible, tunable*

1. INTRODUCTION

Human skin can transduce external stimuli into physiological signals and provide a remarkable network of flexible and stretchable sensors that are highly sensitive to pressure, strain, humidity, and temperature.[1−4] Inspired by human skin, electronic skin (E-skin) is developed to mimic the aforementioned properties using electronic devices and has been found to have wide potential applications, such as wearable devices, prosthetic limbs, health monitoring, remote surgery, robotic skins, and touch interfaces.[5−9] As the particularly important part of E-skin, highly flexible and sensitive pressure sensor is drawing increasing attention. Because of the widespread applications, the highly precise measurement of pressure has become one of the most basic and important requirements in the field of E-skin. These applications of pressure sensors require ultrahigh sensitivity to perceive weak irritants (for instance, the insects crawling), corresponding to subtle-pressure regime (1 Pa to 1 kPa), as well as high flexibility and sensitivity to conformally attach sensors onto the soft and wrinkled human skin (such as monitoring the arterial pulse wave) or to gentle object manipulation of daily activities (such as robot tactile and prosthetic limbs), corresponding to low-pressure regime (1−10 kPa).[10] To date, great progress based on different sensing mechanisms in designing such "skin-like" pressure sensors has been made, including transistor,[11−13] piezoresistive,[14−18] piezoelectric, piezocapacitive,[7,19−21] triboelectric,[22,23] and optical sensing technologies. Among these, pressure sensors based on the piezocapacitive effect play a dominant role owing to the advantage of inherent flexibility, low-power consumption, fast response speed, simple device structure, and low-cost scalable fabrication processes. However, because of the relatively small capacitance change of parallel plates, the capacitive pressure sensors tend to exhibit low sensitivity.[1,10,24]

Received: January 31, 2019
Accepted: March 14, 2019
Published: March 14, 2019

DOI: 10.1021/acsami.9b02049
ACS Appl. Mater. Interfaces 2019, 11, 14997−15006

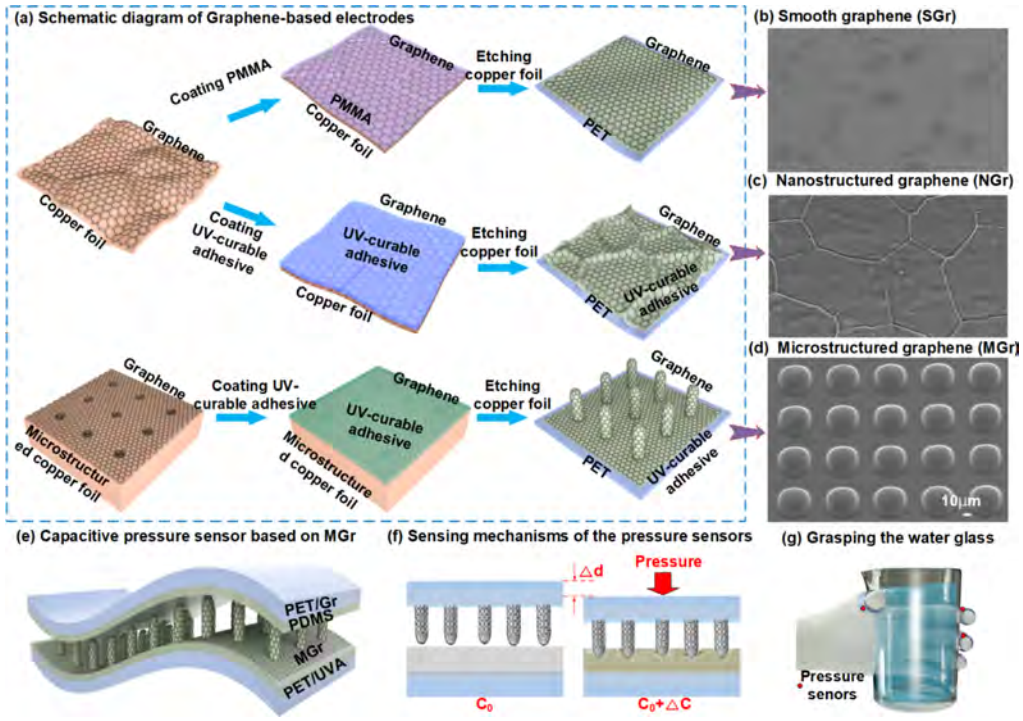

Figure 1. Fabrication of the flexible pressure sensors based on microconformal graphene electrodes. (a) Schematic diagram of fabrication process for different conformal graphene electrodes. (b–d) SEM images of SGrE, NGrE, and MGrE derived from PMMA-based, UVA-based and microconformal transfer methods, respectively. (e) Illustration of capacitive pressure sensor based on MGrE. (f) Schematic diagram of sensing mechanisms. (g) Schematic diagram of grasping with the proposed pressure sensor.

To solve this problem, the conventional solution is to employ microstructured low viscous elastomer (such as polydimethylsiloxane, PDMS) as a dielectric layer. An elastomeric dielectric layer with micropyramid structures was first fabricated by Bao, which greatly improved the sensitivity and response speed.[25,26] In addition, a microporous elastomer has been proved to achieve high sensitivity because of its outstanding compressibility. Cheng et al. proposed hierarchical micropyramid structures to significantly reduce facial hysteresis while remaining its high sensitivity(3.73 kPa^{-1}).[27] Recently, the micropatterned ionic gel-based dielectrics have successfully improved the performance of capacitive pressure sensors and drawn increasing attention.[28−30] Though the sensitivity of capacitive pressure sensors has been enhanced by the microstructured dielectric layers greatly, it is still lower than that of piezoresistive pressure sensors. In recent years, rather than constructing microstructures on dielectric, fabricating flexible microstructured electrodes is a novel effective approach toward a high-sensitive capacitive pressure sensor. Hong and Shuai fabricated the flexible micropatterned silver nanowire (AgNW) electrodes embedded in PDMS with prestrain-induced wrinkling and achieved high-performance pressure sensors.[31−33] Shim et al. developed a low-cost pressure sensor with the rough-paper-based flexible electrode.[34] Guo and co-workers reported a highly sensitive flexible tactile sensor using the bionic micropatterned PDMS−AgNW electrodes replicated from lotus leaves.[35] However, though the process is simple and of low-cost, the preparation of above-mentioned microstructured electrodes are all uncontrollable: (1) both prestrain-induced PDMS wrinkles and replicated bionic microstructures are random, and the characteristic parameters including height, period, and spatial density are uncontrollable, which is difficult for the optimization and regulation of highly sensitive and tunable pressure sensors. For instance, the prestrain-induced PDMS−AgNW electrodes usually endow a relative small height of microstructures (hundreds of nanometers), whereas the morphology of the bionic microstructures is limited for tunability.[25,36] (2) The commonly used conductive electrode materials (mainly AgNWs) are faced with problems in conformability with microstructures to achieve uniform full coverage, which is disadvantageous for improving the sensibility and stability. It is therefore reasonable to construct a controllable and conformal microstructured electrode to improve performance of capacitive pressure sensors.

Herein, we demonstrate a three-dimensional (3D) microconformal graphene electrode with controllable microstructures and perfectly conformal graphene conductive films for ultrasensitive, tunable, and flexible capacitive pressure sensors. Under different fabrication processes of graphene electrodes, multiscale morphologies ranging from nanometers to micrometers have been controllably fabricated for flexible electrodes using the traditional polymethylmethacrylate (PMMA)-mediated transfer method, ultraviolet-curable adhesive (UVA)-mediated transfer method, and microconformal transfer method. Consequently, smooth graphene electrodes (SGrEs), nanostructured graphene electrodes (NGrEs), and microstructured graphene electrodes (MGrE) have been investigated to fabricate the capacitive pressure sensor. It is well known that improving the roughness of electrodes could effectively improve the sensitivity of capacitive pressure sensors, and the sensitivity could be tunable with the controllable microconformal structures. By sandwiching the PDMS dielectric layer between the top MGrE and bottom electrode, we obtained a capacitive pressure sensor with high sensitivity, fast response speed, ultralow detection limit, tunable-sensitivity, high flexibility, and high stability. Furthermore, we demon-

DOI: 10.1021/acsami.9b02049
ACS Appl. Mater. Interfaces 2019, 11, 14997−15006

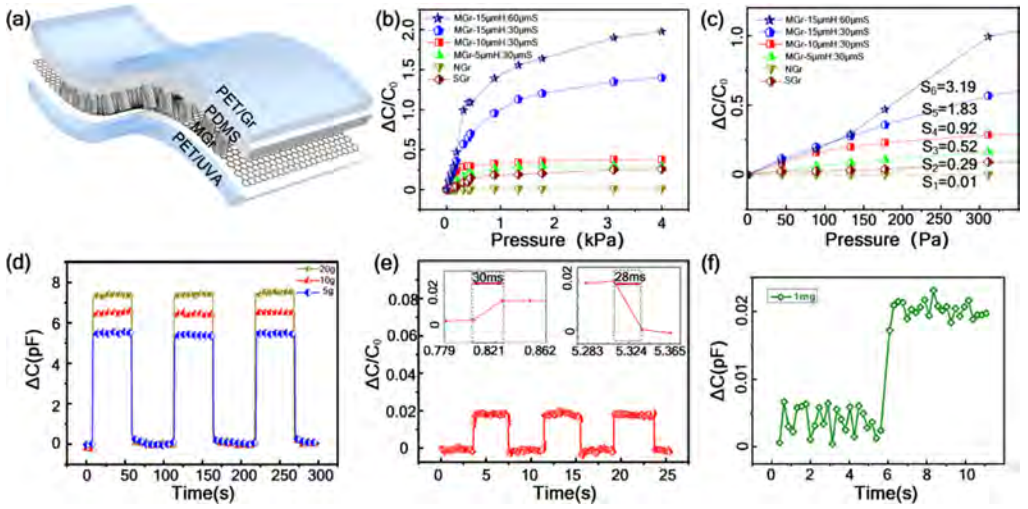

Figure 2. Properties of the MGrE-based sensor. (a) Illustration of pressure sensor based on MGrE. (b) Relative change capacitance of pressure sensor based on various-roughness graphene electrode. (c) Sensitivity of pressure sensor based on various-roughness graphene electrode in subtle-pressure regime. (d) Response of pressure sensor based on MGrE for various loads of 5, 10, and 20 g. (e) The response time of pressure sensor based on MGrE. (f) LOD with an ultralow weight of ∼1 mg.

strate the practical applications including insect crawling detection, wearable health monitoring, and force feedback of robot tactile sensing with a sensor array. This work opens up a new gate to fabricating controllable microstructured electrodes to enhance the performance of capacitive pressure sensors.

2. RESULTS AND DISCUSSION

2.1. Preparation and Characterization. Figure 1a illustrates the process of fabricating different structured electrodes. Three kinds of flexible graphene electrodes (smooth, nanostructured, and microstructured) were controllably fabricated via traditional PMMA-mediated transfer method, UVA-mediated transfer method, and microconformal transfer method, respectively.

2.1.1. Smooth Graphene Electrodes. Following the traditional PMMA-mediated transferring method to transfer chemical vapor deposition (CVD) graphene onto polyethylene terephthalate (PET) substrate,[37,38] we obtained relatively SGrEs with a small root-mean-square roughness (R_{rms}) about 10 nm (Figures 1b and S3a). In this method, a 100 nm thick PMMA layer is spin-coated onto the CVD-grown copper/graphene, and the copper below it is etched away completely by an etchant. The PMMA/graphene stack is subsequently transferred onto a flexible 100 μm-thick PET substrate, and hot acetone solvents are used to remove the PMMA sacrificial layer. As reported in our previous work,[39] the graphene wrinkles and grain boundaries that originated from high-temperature recrystallization of copper foils obviously exists in PET/graphene, as shown in Figure 1b. The annealing and growing temperature of CVD graphene (950−1050 °C) is far above the copper recrystallization temperature of ∼227 °C,[40] causing the formation of copper grain boundaries (Figure S1a,b). As shown in Figure S1c,d, the depth of copper grain boundaries is up to 346.4 nm and the R_{rms} of CVD-grown copper/graphene is ∼65.6 nm. However, after the PMMA-mediated transfer, the R_{rms} of PET/graphene is below 3 nm (Figure S2a,b). The reduction of roughness is due to the removal of PMMA sacrificial layer (or support layer), which leads to the collapse of graphene. Apparently, leaving the support layer on can maintain the nanostructure of grain boundaries, which is beneficial to high sensitivity of capacitive pressure sensors.

2.1.2. Nanostructured Graphene Electrodes. To retain the nanostructured grain boundaries, an UVA was adopted as a transfer medium and support layer, which was introduced in our recent report.[36] The liquid UVA prepolymer was drop-coated onto the copper/graphene surface, followed by lamination of a 100 μm-thick PET, and cured in the exposure of 365 nm UV light (10 mW/cm^2, 5 min). After the copper film is etched away, instead of removing the transfer medium, both the UVA layer filled in the grain boundaries and PET film served as the substrate for graphene electrodes. The graphene film conformally covers the UVA support layer, and the NGrEs are achieved with the roughness of R_{rms} ≈ 82.3 nm and the height of grain boundaries up to 400 nm (Figures 1c and S2). Both roughness of NGrE and height of boundaries are higher than those of copper/graphene (R_{rms} ≈ 65.6 nm and height ≈ 346.4 nm), which is mainly due to that the atomic force microscopy (AFM) tip cannot detect the bottom of copper grain boundaries.

2.1.3. Microstructured Graphene Electrodes. To obtain controllable roughness that is larger than nanoscale of electrodes with a conformal graphene film, a systematic research by means of photolithography and the wet etching microfabrication process was adopted.[41,42] In detail, we fabricated a microstructured copper foil to get MGrEs via 3D conformal growth. In this paper, the period, duty ratio, and height were well designed. First, as depicted in Figure S3, the copper foil was patterned into microstructure with rectangular holes by UV lithography and etching. After isotropic wet etching and high-temperature melting during CVD process, the microstructure of copper was reconstructed into an inverse-dome shape, as shown in Figure S4a,b. With aforementioned UVA-mediated transfer method including UVA coating, UV-curing, and copper etching, the MGrEs are comformally fabricated on the PET substrate (Figures 1d and S4c).

As shown in Figure S4d−f in the Supporting Information, the microcylinder arrays with different height are regular and uniform. The uniformity of microstructures guarantees uni-

DOI: 10.1021/acsami.9b02049
ACS Appl. Mater. Interfaces 2019, 11, 14997−15006

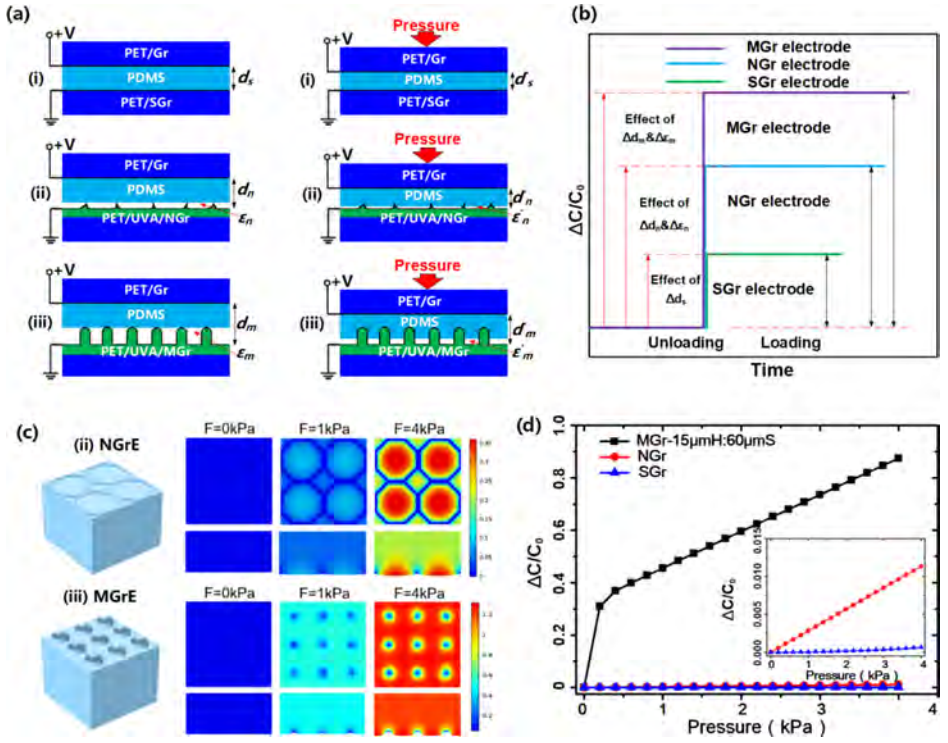

Figure 3. Sensing mechanisms of the MGrE-based sensors. (a) Graphical explanation of capacitive pressure sensor based on SGrE, NGrE, and MgrE and their corresponding geometrical change during the process of loading pressure, respectively. (b) Relative capacitance variations of pressure sensors based on the three kinds of electrodes induced by identical levels of external pressure. (c) Finite-element simulation showing the local stress distribution and the deformation of NGrE and MGrE. (d) Simulated change in displacement of three structures under applied.

form distribution of pressure and decrease random error of measurement. Note that the height is controlled by the etching time and the diameter of microcylinder will be increased with the increasing etching time. To measure the height of microstructures, laser scanning confocal microscopy (LSCM) was adopted to characterize the large height above 15 μm, which is beyond the limit of an atomic force microscope. Figure S5 shows the 3D morphology of MGrEs on PET/UVA, and the heights that resulted from different etching times are about 5, 10, and 15 μm, respectively, which are 3 orders higher than that of SGrE and 1 order higher than that of NGrE. The graphene was confirmed as a single layer via the Raman spectrum, as shown in Figure S6 in the Supporting Information. The specific ratio of 2D peak intensity to G peak intensity (I_{2D}/I_G) is ~2, which indicates that the graphene of MGrE is a monolayer.[43] Weak D peaks manifest that this graphene conformal transfer method is of high-quality, effective, and reliable.

2.2. Basic Sensing Properties. The sensing performance of the flexible capacitive pressure sensors based on three kinds of flexible graphene electrodes (SGrE, NGrE, and MGrE) is demonstrated in Figure 2. To investigate the effect of the microstructured electrodes on sensing performance, as shown in Figure 2a, the sandwiched pressure sensor uses a microstructured graphene electrode as the bottom electrode, flat PDMS dielectric layer, and smooth graphene on the PET substrate as the top electrode. The thickness of the dielectric layer is about 150 μm, and the smooth graphene on PET is fabricated via the traditional PMMA transfer method. The microstructures and morphologies of the bottom electrode include SGrE (height of ~20 nm), NGrE (height of ~400 nm), and MGrE with different heights from 5 to 15 μm. We compared the sensitivity of pressure sensors with different morphologies of the bottom electrodes (Figure 2b). The sensitivity of capacitive pressure sensor is given by

$$S = \delta(\Delta C/C_0)/\delta P \quad (1)$$

where P is the applied pressure, C and C_0 are the capacitances with and without pressure, respectively, and ΔC is the relative change of capacitance ($C-C_0$). On the basis of the equation, we can calculate the sensitivity of the pressure sensors through the tangent of the curve of capacitance variation versus loading pressure. As we expected, the sensitivity increases with the increase of roughness. Thereinto the capacitive pressure sensor with highest microstructure has the largest sensitivity (3.19 kPa^{-1}), which is 319 times higher than that of SGrE-based sensor, 11 times higher than that of NgrE-based sensor, 5.8 times higher than the sensitivity of Bao's structured PDMS layer (0.55 kPa^{-1}),[26] and higher than that of previous micropatterned electrodes (1.194, 2.94 kPa^{-1}).[29,34] The capacitance of highest microstructure rises from 9.43 to 28.3 pF when pressure increases from 0 to 4 kPa. In addition, the sensitivity of microstructured pressure sensors in the second linear range is also the largest, which resulted from that the increasing height of electrode makes it easier to penetrate into the dielectric layer.

To investigate the tunable-sensitivity of the pressure sensor, we fabricated devices with various characteristic parameters of microstructured graphene electrodes including three kinds of height (H: 5, 10, and 15 μm) and two kinds of space densities (S: 30 and 60 μm). As illustrated in Figure 2b–c, the sensitivity increases from 0.52 to 1.83 kPa^{-1} as the height increases from 5 to 15 μm. The highest height endows the largest compressibility under the same loading pressure. On

DOI: 10.1021/acsami.9b02049
ACS Appl. Mater. Interfaces 2019, 11, 14997–15006

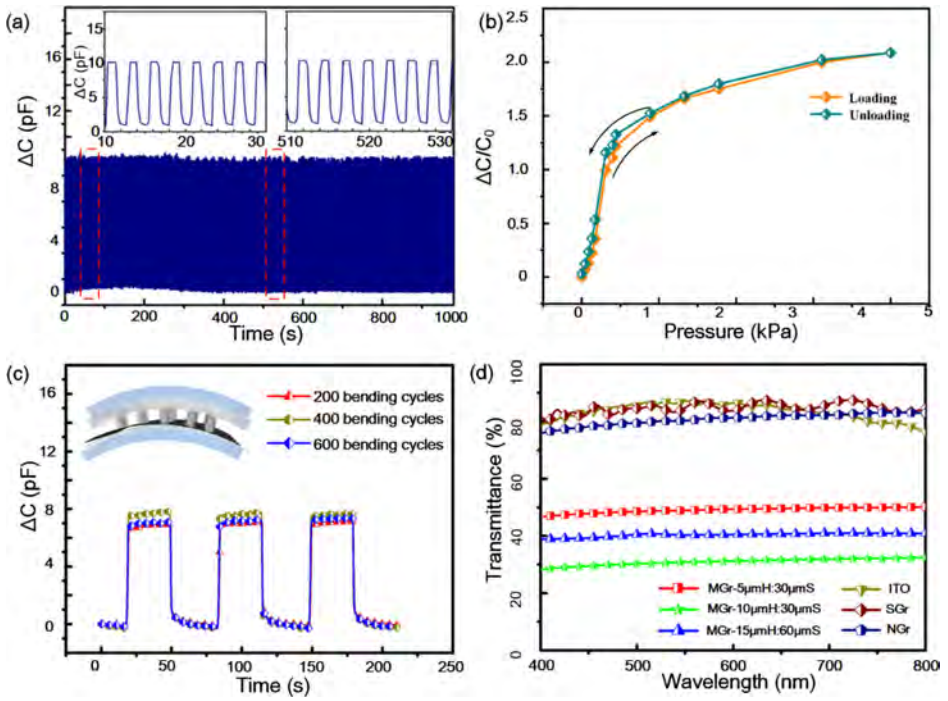

Figure 4. (a) Stability of capacitive response for the pressure sensor with sparse patterns under a load over 500 cycles. (b) Relative capacitance changes of two consecutive loading and unloading cycles for the pressure sensor. (c) Flexibility measurement under different bending cycles. (d) Optical transmittance as a function of wavelength for different flexible transparent electrodes.

the other hand, the space density plays an important role in improving the sensitivity. It is obviously shown that the sensitivity of the device with sparse microstructures (3.19 kPa^{-1}) is higher than that of one with dense microstructures (1.83 kPa^{-1}), which is similar to previously reported works.[25,35,36] It could be understood that, for sparse microstructured electrodes, each microcylinder suffers from bigger loading pressure than the dense case and the sparse MGrE tends to be compressed easily.

To evaluate the repeatability of the sensors, piezocapacitance analysis of time for three cycles of applied load of 5 g (220 Pa), 10 g (440 Pa), and 20 g (880 Pa) was conducted and reveals that the MGrE sensor exhibits a real-time and rapid dynamic response performance (Figure 2d). Repeatable and stable pressure-sensing behaviors under various loads were studied, wherein the capacitance of the MGrE sensor changes sharply with pressure loading and unloading. The results show that the MGrE sensor presents stable responses with a high sensitivity and great repeatability.

We have subsequently investigated the response time for the MGrE-based capacitive pressure sensors. Response time and recovery time are important factors of flexible pressure sensors that must be considered to minimize the response hysteresis of the sensor. Figure 2e shows the response and recovery time of the MGrE sensor with pressure loading and unloading. When loaded with pressure, the capacitance of the MGrE sensor rapidly ascends within a fast response time of 30 ms, which is superior to the response time of human skin (30−50 ms),[43,44] and then stays at a stable value. After the loading force is removed, the capacitance of the MGrE sensor decreases promptly in a short recovery time about 28 ms and thereafter attenuates to its initial value (see the inset of Figure 2e). The response time and recovery time of the MGrE sensors are shorter than those of traditional polymer-based flexible tactile sensors which exhibit severe viscoelastic behavior.[21] The difference between the response time and recovery time might be ascribed to that loading is slower than unloading.

More importantly, to demonstrate the limit of detection (LOD) for the MGrE-based capacitive pressure sensor, an ultrasmall weight of slight paper (1 mg) was uniformly loaded on the MGrE sensor. In addition, as is depicted in Figure 2f, the piezocapacitance response is clearly distinguishable and the microconformal graphene electrode endows the device with an extremely low limit of pressure detection.

2.3. Sensing Mechanism. The pressure-sensing mechanism behind the capacitive pressure sensors based on three kinds of conformal graphene electrodes are schematically illustrated in Figure 3. For capacitive pressure sensors, the variation rate of capacitance depends on the relative dielectric parameters of multilayered materials and the electrode distance according to the definition of generalized parallel-plate capacitance $C \propto A\varepsilon_r\varepsilon_0/d$, where ε_r and ε_0 are the relative dielectric parameter of the material and the permittivity of air, d is the distance between two electrodes, and A is the effective area of the two electrodes. The area (A) of planar plate capacitor is considered as constant while outside pressure is loaded onto the sensor, and the compressibility of dielectric materials has a significant effect on the sensitivity due to the remarkable change of distance between upper and bottom electrodes. Compared with the SGrE-based (type i) and NGrE-based (type ii) capacitive pressure sensor, under the same external loading, the MGrE-based sensor (type iii) shows larger deformation. Figure 3a illustrates the schematic diagram for the relative capacitance variation to the corresponding deformation behaviors. It is obvious that the MGrE-based sensor endows the largest deformation (Δd). In addition, the shrinking of the air gap existing between the MGrE and dielectric layer will lead to the increasing of the effective permittivity ($\Delta\varepsilon$), which observably improved the pressure sensitivity. Figure 2b depicts the response of pressure loading-

DOI: 10.1021/acsami.9b02049
ACS Appl. Mater. Interfaces 2019, 11, 14997−15006

capacitance for three types of sensors. It is observed that the sensor with MGr electrode has a more remarkable loading response $\Delta C/C_0$ than those of the NGr electrode and SGr electrode, exhibiting higher sensitivity with the identical applied force.

To explore the sensor mechanism, we employ the finite element analysis (FEA) to simulate the deformation of different multilayered microstructures. The FEA is performed with a COMSOL Multiphysics 5.3a software system. The displacement of the compliant PDMS layer between electrode interfaces are obtained when increasing the applied pressure from 0 to 4 kPa. The simulation results of two types of conformal microstructure electrodes (NGrE and MGrE) are illustrated in Figure 3c. First, we equivalently modeled the graphene grain boundary as a polygon feature according to the scanning electron microscopy (SEM) graphs and also gave one of representative truncated pillar microstructures with nine element microstructures in the same area. Then, we obtained the displacement field distribution on the electrode interface when different pressures were applied. It is seen that the better compressibility of MGrE causes larger change of separation between electrodes and thus provides higher sensitivity than NGrE- and SGrE-type sensors. Finally, we also obtained the electromechanical coupling behavior of different microstructured sensor with the increasing pressure, as shown in Figure 3d. The results demonstrate that the change rate $\Delta C/C_0$ of the MGr-15 μmH:60 μmS type pressure sensor is significantly higher than those of other two types of sensors and thus shows superior sensitivity than previous capacitive sensors with similar microstructure forms. When manufacturing large-area pressure sensors, the higher sensitivity of these MGrE-based pressure sensors can be good potential in applications of electric skins and smart wearables.

2.4. Stability and Bendability of the Device. For practical applications, high stability and robustness are also very important. We have also investigated the endurance of the flexible capacitive pressure sensor by repeatedly loading/unloading a pressure for 500 cycles. As shown in Figure 4a, the fabricated sensor well maintains its pressure-sensing behavior without showing obvious degradation during the test. The insets in Figure 4a show signals under two different stages of repeated testing, exhibiting quite similar waveforms, and the results indicate that during the 1000 cycles of loading/unloading, no fatigue appears. This demonstrates that under harsh pressure conditions, little or no fatigue occurs in microconformal graphene electrodes, which confirms the durability of the MGrE-based tactile sensors. Furthermore, the hysteresis of the MGrE sensor under consecutive loading and unloading cycle from 0 to 4 kPa is conducted with the piezocapacitance response curves. As shown in Figure 4b, the hysteresis is much smaller than that of the previously reported capacitive pressure sensors, indicating a strong robustness.

To explore the performance of the microstructured graphene electrodes in flexible transparent wearable devices, the bending stability and transmittance were carried out. Figure 4c shows the pressure response of the MGrE sensor after 200, 400, and 600 bending times, where the bending radius is ~10 mm. Because of the excellent mechanical property of graphene, the signal is stably maintained and returns to the initial value as the sensor goes to the nonbent status. The response to bending is attributed to the in-plane tensile and compressive stresses in the sandwiched structure.[29] Therefore, the MGrE sensor is bendable for wearable devices or robot tactile sensing. On the other hand, the transmittance is investigated in Figure 4d. Compared with the traditional ITO electrode, both SGrE-based sensor and NGrE-based sensor possess high transparency up to 90%, whereas the MGrE-based sensors possess relatively low transparency below 50% because of light scattering caused by the microstructures.

2.5. Ultrasensitivity of Double-MGrE-Based Sensor. Furthermore, to improve the sensitivity of the MGrE sensor, a symmetric sandwiched piezocapacitance sensor with double microstructured electrodes as both the bottom and top electrodes is illustrated in Figure 5a. Expectedly, a high

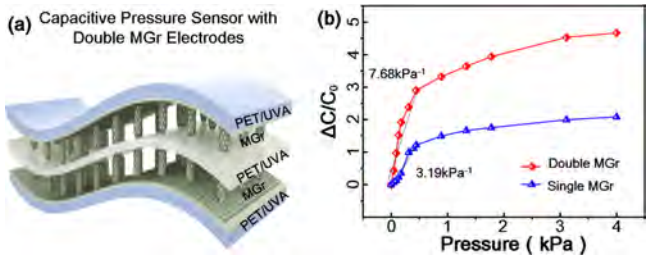

Figure 5. (a) Schematic diagram of capacitive pressure sensor with double MGrEs. (b) Relative capacitance curve for two kinds of pressure sensors with single MGrE and double MGrEs against increasing pressure.

sensitivity of 7.68 kPa^{-1} is obtained for the pressure sensor with double microstructured electrodes in low-pressure region, as shown in Figure 5b. The sensitivity of pressure sensor with single microstructured electrode (3.17 kPa^{-1}) is around half of that in pressure sensor with double microstructured electrodes. From this comparison, we can observe that micropattern of electrodes plays a crucial role to the sensitivity of a capacitive pressure sensor, and the sensitivity enhancement for microstructured electrodes can be accumulated.

2.6. Applications of Single Sensor. As mentioned above, the proposed MGrE-based pressure sensors possess a very excellent sensitivity, ultralow LOD, and high stability, which is of great potential for widespread applications, such as ultralow-pressure monitoring, biological research, and wearable human-health monitoring. Figure 6a illustrates the response of an insect's crawling on the top of pressure sensor. To successfully capture each crawling process, we trapped the insect into a Petri dish, and the insect can crawl freely in this region. When the insect crawls through the pressure sensor, we can monitor every step of the insect's crawling. The first step and final step is a state of climbing on and leaving the sensor, respectively, which have bigger force loads than other steps on pressure sensor. As a consequence, the relative capacitance change of these two steps will be larger than the other three steps. By this experiment, the MGrE-based pressure sensors is proved to be able to detect tiny movements of insects and thus helpful for some biological research. Figure 6b illustrates the capacitance response to the applied pressure induced by water droplets of 15 mg per drop. The MGrE-based sensor is highly sensitive and fast responding to external ultralow load, and the stepped incrment of the capacitance variation is primarily corresponding to the accumulation process of water droplets on the sensor.

In addition, we further investigate the possibility of MGrE-based sensor for wearable human-health monitoring. As is well known, cardiovascular disease is a worldwide leading cause of death, and the continuous monitoring of radial artery pressure

DOI: 10.1021/acsami.9b02049
ACS Appl. Mater. Interfaces 2019, 11, 14997−15006

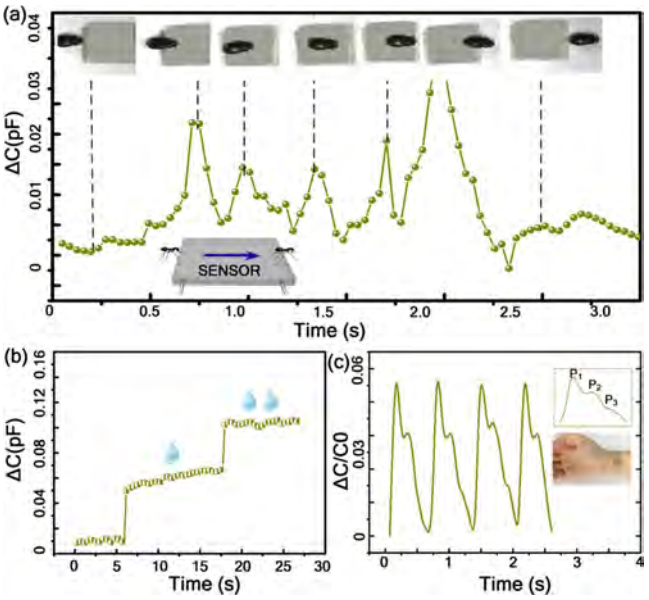

Figure 6. (a) Response of an insect's crawling on the top of pressure sensor. Insets are the photographs of insect's crawling process. (b) Performance of the pressure sensor device induced by droplets of water falling. (c) Performance of blood pressure monitoring using a pressure sensor.

is a noninvasive and real-time method for diagnosis.[45,46] Figure 6c illustrates wrist pulse waves monitoring an application and our MGrE-based sensor was attached onto the wrist of a volunteer via a scotch tape. The typical pulse waveform with three peaks P_1, P_2, and P_3 was successfully obtained, which is essential to extract the blood pressure. Therefore, the proposed MGrE-based sensor shows promising potential in real-time health monitoring.

2.7. Spatial Distinguishing Ability of a Sensor Array. Single pressure sensor is limited for practical application because it is only able to detect the applied pressure of one "point" but without spatial resolution. The sensor array can enable the pressures mapping with spatial resolution like real human skins, which is important for human−machine interaction, robot tactile, and other artificial intelligence. Figure 7a illustrates a 3 × 3 multipixel sensor array based on a flexible printed circuit for readout. A circuit board for the capacitive sensor array consisted of analog devices capacitance-to-digital converter (CDC) chip and a microcontroller was adopted, and the changes of capacitance can be converted into voltage signals. To measure the spatial pressure resolution, three different weights (20, 50, and 100 g) were placed on the unit 1B, 3C, and 2A of the proposed sensor array, respectively. A 3D distribution graph of pressure mapping in Figure 7b illustrates that the highest response locates at the unit 2A, where the largest weight of 100 g is placed. Consequently, the rest of 1B and 3C shows relatively small capacitance variations. These results indicate that our fabricated MGrE-based capacitive sensors can be integrated into arrays and realize the pressure mappings and be of great potential applications in intelligent robots.

2.8. Force Feedback of Robot Tactile Sensing. Human-like robot tactile sensing is highly desired in artificial intelligence, service robots, industrial robots, surgical robots, and artificial limbs.[47] To demonstrate the potential for the robot tactile applications, five proposed sensors were integrated into a smart tactile glove, as illustrated in Figure 7c−e. The sensors were sticked to five fingers of the glove to achieve the force feedback of different weights during grasping objects. Herein, three different weights on glass cup with empty, 250 mL water, and 500 mL water were conducted in the grasping tasks. Depending on the active areas of the sensors that covered with objects, we observed different changes of

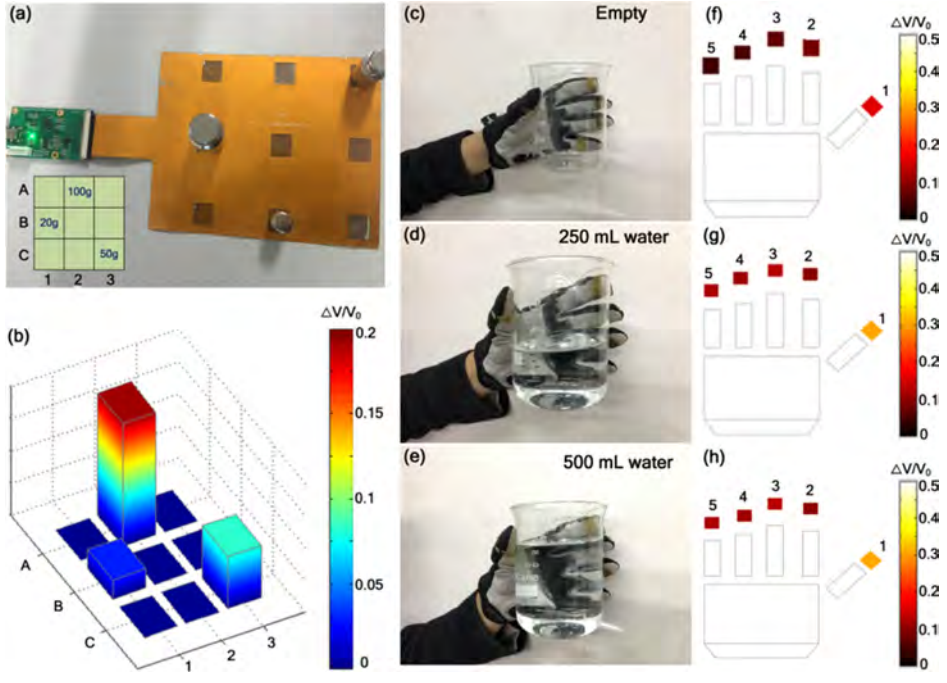

Figure 7. (a,b) Photograph of 3 × 3 pixels pressure sensor array with loading three weights and the corresponding 3D signal intensity and distribution. (c−e) Photographs of subjects grasping with the different amount weights. (f−h) Graphics shows the change in capacitance values when the subject grasps the different amount weights.

DOI: 10.1021/acsami.9b02049
ACS Appl. Mater. Interfaces 2019, 11, 14997−15006

readout voltages measured at each sensor. Comparing the readout voltages among three grasping tasks, we can observe that change in voltage values among the sensors is found to be the highest when grasping the heaviest object (500 mL water). Interestingly, in each grasping situation, the sensor in the thumb finger endows the largest readout voltage, which is consistent with the grasping habit of human beings. Our demonstration is an evidence that the MGrE-based flexible sensors can be used to reflect the fingertip pressure level during a grasping action and deserve wide applications for robotic control and human−machine interaction.

3. CONCLUSION

In summary, we have demonstrated a novel and controllable microstructured graphene electrode for ultrasensitive and tunable flexible capacitive pressure sensors. Benefited from the 3D microconformal graphene, multiscale roughness ranging from a few nanometers to hundreds of nanometers and to tens of micrometers have been systematically investigated to improve the sensitivity of device. By sandwiching the PDMS dielectric layer between the top microstructured graphene electrode and the bottom electrode, the high-performance capacitive pressure sensor was obtained with high sensitivity (3.19 kPa^{-1}), fast response speed (30 ms), ultralow detection limit, tunable-sensitivity, high flexibility, and high stability. Besides, an ultrasensitivity of 7.68 kPa^{-1} was achieved via a symmetric sandwiched sensor with double MGrE as both the bottom and top electrodes. It is evident that the microstructured graphene electrode can effectively improve the sensitivity of capacitive pressure sensors and the sensitivity can be tunable with the controllable microconformal structure. The finite element analysis (FEA) method has been carried out to simulate the sensing process, and the contact area and compressibility of the microstructured surface determine the piezocapacitive response. Owing to its high sensitivity and fast response speed, the proposed pressure sensor has an ultralow LOD and successfully verifies the potential applications including insect crawling detection and wrist pulse waves monitoring. We have also presented that the microstructured graphene electrodes can be utilized in the application of pressure distribution with the sensor array and force feedback of robot tactile sensing.

4. EXPERIMENTAL SECTION

4.1. Fabrication of SGrEs. A 1.5 cm × 1.5 cm polycrystalline copper foil was used in the graphene growth by CVD. Polymethyl methacrylate (4 wt % dispersion in ethyl lactate) solution was spin-coated on a graphene/copper foil. The spin-coating speed was about 3000 rpm. After coating, it should be baked at 170 ° for 10 min. Next, the copper foils were etched by a mixed etchant (10 mL hydrochloric acid and 5 mL hydrogen peroxide dispersion in water) for 5 h. Then, the floating graphene was washed in deionized water and transferred to PET. Finally, the SGrE was achieved after removing the PMMA coating in acetone.

4.2. Fabrication of NGrEs. A 1.5 cm × 1.5 cm polycrystalline copper foil was used in the graphene growth by CVD. Then, UV-curable adhesives were drop-coated onto copper foil and PET was put on the uncured UV-curable adhesives. The UV-curable adhesives were cured in the exposure of UV light for 5 min. A mixed etchant (10 mL hydrochloric acid and 5 mL hydrogen peroxide dispersion in water) was used to etch copper foil and graphene electrode with a structure conformal with the grain was obtained.

4.3. Fabrication of MGrEs. A 1.0 cm × 1.0 cm polycrystalline copper foil was coated by photoresist (AZ 9260) and baked under 100 °C for 10 min. The coated copper foil was exposed under the UV light for 20 s and was developed by a developing solution (AZ 400K). Then, the patterned copper foil was etched by an etchant (1 mol/L ferric chloride solution) to get the microstructure. The depth of microstructure was decided by etching time. Next, a microstructured copper foil was used in graphene growth by CVD. Then, UV-curable adhesives were used to transfer graphene, which was conformal with the microstructured copper foil, to the PET film. First the microstructured copper foil was fabricated by photolithography. Thereinto the etchant was $FeCl_3$ solution (1 mol/L), and preparation of $FeCl_3$ solution needed dissolving $FeCl_3$ bulk into boiling water. Next, CVD was used to grow graphene on the microstructured copper foil. In the end, UV-curable adhesives were used to transfer the graphene to PET and keep the microstructure of graphene on the PET. On the basis of the microstructured graphene electrode, we fabricated a highly sensitive and flexible pressure sensor.

4.4. Fabrication of Graphene-Based Pressure Sensor. The graphene-based top electrodes with a size of 1.5 × 1.5 cm^2 was laminated onto the same-sized micropatterned bottom electrodes with a PDMS dielectric layer facing the micropatterns. The copper wire was mounted on the terminal of graphene electrode. The PDMS film (∼150 μm) was fabricated using PDMS prepolymer and the base-to-curing-agent with the ratio of 10:1. After being degassed under vacuum, the prepolymer was drop-casted onto a slide glass and cured at 80 °C for 1 h. For the tactile sensors, the fabricated PDMS films were cut into pieces with a size of 1.5 × 1.5 cm^2. For the assembled MGrE pressure sensors, they had a 1.5 × 1.5 cm^2 pressure-sensing area between the PDMS film and graphene-based electrode layer on the physically stacked structure. Finally, the edges were bonded together using 3M Scotch tape to assemble the sandwich-structure tactile sensor.

4.5. Characterization. The surface morphologies of the micro-/nano-structured graphene electrodes were analyzed by field-emission SEM (JEOL JSM-7800F) with a 5 kV accelerating voltage. In addition, 3D morphologies and heights of microstructures were performed on a LSCM (OLYMPUS 4000s). The Raman spectra of microconformal graphene were verified by Raman spectroscopy measurements (Renishaw inVia Reflex) with a laser excitation wavelength of 532 nm and spot diameter of ∼1 μm. The optical transmittance spectra of graphene electrodes were obtained using a UV−vis spectrophotometer (PerkinElmer, Lambda 35). In addition, the capacitance of the pressure sensor was measured by a Keithley 4200A parameter analyzer (4200A-SCS). We linked our device to the Keithley 4200A parameter analyzer and used a capacitance voltage measurement unit to measure the capacitance of our device at 100 kHz with a 0.1 V alternating current signal at room temperature in air. A thin glass slide (10 mm × 15 mm, 250 mg) was placed on the surface of the sensor device before pressure measurement. For the pressure measurement, a force gauge with computer-controlled stage (XLD-20E, Jingkong Mechanical testing Co., Ltd) was adopted, and the magnitude and frequency of the force were controlled by measurement system. For cyclic loading/unloading testing, the sensor was placed on the testing system, and a preselected constant pressure was repeatedly applied and released using the force gauge (tip diameter: 10 mm).

4.6. Finite Element Analysis. A 3D model and numerical simulations were performed using COMSOL Multiphysics (V5.3a). The original height and diameter of microcylinder were 15 and 10 μm, respectively. To simplify the simulation processes, the graphene film was ignored, and the UVA was set as PET. The Young's modulus values of PET and PDMS were set as 3.5 GPa and 2 MPa, respectively, with Poisson's ratios of 0.4 and 0.49 for PET and PDMS. The gradual load increased from 0 to 4 kPa was applied to the top of PET layer.

4.7. Array Circuit. The circuit board for the capacitive sensor array consists of an analog device CDC chip (AD7144, Analog Devices) and a microcontroller (STM32FO, ST Microelectronics). The CDC was essentially a delta-sigma analog-to-digital converter. In this case, a constant voltage input was used, whereas the feedback capacitor of the integrator was the sense capacitor. AD7144 offers 14 channels, 16-bit resolution, a configurable test range, and excellent

DOI: 10.1021/acsami.9b02049
ACS Appl. Mater. Interfaces 2019, 11, 14997−15006

linearity. The low-power microcontroller controlled the CDC and transmitted the measured capacitance data through a serial port into a computer where digital values of the capacitance could be acquired and displayed. The overall system was operated with a supply voltage of 3.3 V, powered by a USB. The entire 3 × 3 array of nine sensors was sampled 3 times per second.

■ ASSOCIATED CONTENT

Supporting Information

The Supporting Information is available free of charge on the ACS Publications website at DOI: 10.1021/acsami.9b02049.

Fabrication process of microstructured graphene on copper foil; SEM images of microstructured graphene film on cooper; AFM images of nanostructured graphene film on cooper; AFM image of graphene film on PET via PMMA-assisted transfer method; AFM image of graphene film on PET via UVA-assisted transfer method; SEM images of microstructured graphene film on cooper; SEM images of microstructured graphene film on PET with different etching time for 5 μm high microcylinder, 10 μm high microcylinder, and 15 μm high microcylinder arrays; LSCM 3D images of microstructured graphene film on PET with different etching time for 5 μm high microcylinder, 10 μm high microcylinder, and 15 μm high microcylinder arrays via UVA-assisted transfer method; sectional images of microstructured graphene film on PET with different etching time for 5 μm high microcylinder, 10 μm high microcylinder, and 15 μm high microcylinder arrays; and Raman spectra of microconformal CVD graphene electrodes (PDF)

■ AUTHOR INFORMATION

Corresponding Authors

*E-mail: weidong.yang@nus.edu.sg (W.Y.).
*E-mail: dpwei@cigit.ac.cn (D.W.).

ORCID

Jun Yang: 0000-0003-1652-0054
Dapeng Wei: 0000-0002-3575-617X

Author Contributions

J.Y. and S.L. contribute equally to this work. The manuscript was written through contributions of all authors. All authors have given approval to the final version of the manuscript.

Notes

The authors declare no competing financial interest.

■ ACKNOWLEDGMENTS

This work was supported by the National Natural Science Foundation of China (NSFC 61504148), the Basic Science and Frontier Technology Research Program of Chongqing (cstc2016jcyjA0315, cstc2017shmsA50001), Youth Innovation Promotion Association of CAS (2015316), Project of Chongqing brain science Collaborative Innovation Center, Project of CAS Western Young Scholar, Project of CQ CSTC (cstc2017zdcy-zdyfX0001).

■ REFERENCES

(1) Chortos, A.; Liu, J.; Bao, Z. Pursuing Prosthetic Electronic Skin. *Nat. Mater.* **2016**, *15*, 937−950.
(2) Chou, H.-H.; Nguyen, A.; Chortos, A.; To, J. W. F.; Lu, C.; Mei, J.; Kurosawa, T.; Bae, W.-G.; Tok, J. B. H.; Bao, Z. A Chameleon-inspired Stretchable Electronic Skin with Interactive Colour Changing Controlled by Tactile Sensing. *Nat. Commun.* **2015**, *6*, 8011.
(3) Hua, Q.; Sun, J.; Liu, H.; Bao, R.; Yu, R.; Zhai, J.; Pan, C.; Wang, Z. L. Skin-inspired Highly Stretchable and Conformable Matrix Networks for Multifunctional Sensing. *Nat. Commun.* **2018**, *9*, 244.
(4) Nela, L.; Tang, J.; Cao, Q.; Tulevski, G.; Han, S.-J. Large-Area High-Performance Flexible Pressure Sensor with Carbon Nanotube Active Matrix for Electronic Skin. *Nano Lett.* **2018**, *18*, 2054−2059.
(5) Tao, L.-Q.; Tian, H.; Liu, Y.; Ju, Z.-Y.; Pang, Y.; Chen, Y.-Q.; Wang, D.-Y.; Tian, X.-G.; Yan, J.-C.; Deng, N.-Q.; Yang, T.-L. Intelligent Artificial Throat with Sound-sensing Ability Based on Laser Induced Graphene. *Nat. Commun.* **2017**, *8*, 14579.
(6) Ye, D.; Ding, Y.; Duan, Y.; Su, J.; Yin, Z.; Huang, Y. A. Large-Scale Direct-Writing of Aligned Nanofibers for Flexible Electronics. *Small* **2018**, *14*, 1703521.
(7) Wu, F.; Chen, S.; Chen, B.; Wang, M.; Min, L.; Alvarenga, J.; Ju, J.; Khademhosseini, A.; Yao, Y.; Zhang, Y. S.; Aizenberg, J.; Hou, X. Bioinspired Universal Flexible Elastomer-Based Microchannels. *Small* **2018**, *14*, 1702170.
(8) Pu, X.; Guo, H.; Chen, J.; Wang, X.; Xi, Y.; Hu, C.; Wang, Z. L.; Hu, W.; Wang, Z. L. Eye motion triggered self-powered mechnosensational communication system using triboelectric nanogenerator. *Sci. Adv.* **2017**, *3*, No. e1700694.
(9) Byun, J.; Lee, Y.; Yoon, J.; Lee, B.; Oh, E.; Chung, S.; Lee, T.; Cho, K.-J.; Kim, J.; Hong, Y. Electronic Skins for Soft, Compact, Reversible Assembly of Wirelessly Activated Fully Soft Robots. *Sci. Rob.* **2018**, *3*, No. eaas9020.
(10) Zang, Y.; Zhang, F.; Di, C. A.; Zhu, D. Advances of Flexible Pressure Sensors toward Artificial Intelligence and Health Care Applications. *Mater. Horiz.* **2015**, *2*, 140−156.
(11) Zang, Y.; Zhang, F.; Huang, D.; Gao, X.; Di, C.; Zhu, D. Flexible Suspended Gate Organic Thin-film Transistors for Ultra-sensitive Pressure Detection. *Nat. Commun.* **2015**, *6*, 6269.
(12) Wang, C.; Hwang, D.; Yu, Z.; Takei, K.; Park, J.; Chen, T.; Ma, B.; Javey, A. User-interactive Electronic Skin for Instantaneous Pressure Visualization. *Nat. Mater.* **2013**, *12*, 899−904.
(13) Takei, K.; Takahashi, T.; Ho, J. C.; Ko, H.; Gillies, A. G.; Leu, P. W.; Fearing, R. S.; Javey, A. Nanowire Active-matrix Circuitry for Low-voltage Macroscale Artificial Skin. *Nat. Mater.* **2010**, *9*, 821−826.
(14) Wu, H.; Liu, Q.; Du, W.; Li, C.; Shi, G. Transparent Polymeric Strain Sensors for Monitoring Vital Signs and Beyond. *ACS Appl. Mater. Interfaces* **2018**, *10*, 3895−3901.
(15) Mu, C.; Song, Y.; Huang, W.; Ran, A.; Sun, R.; Xie, W.; Zhang, H. Flexible Normal-Tangential Force Sensor with Opposite Resistance Responding for Highly Sensitive Artificial Skin. *Adv. Funct. Mater.* **2018**, *28*, 1707503.
(16) Wang, Q.; Jian, M.; Wang, C.; Zhang, Y. Carbonized Silk Nanofiber Membrane for Transparent and Sensitive Electronic Skin. *Adv. Funct. Mater.* **2017**, *27*, 1605657.
(17) Liu, Q.; Chen, J.; Li, Y.; Shi, G. High-Performance Strain Sensors with Fish-Scale-Like Graphene-Sensing Layers for Full-Range Detection of Human Motions. *ACS Nano* **2016**, *10*, 7901−7906.
(18) Roh, E.; Hwang, B.-U.; Kim, D.; Kim, B.-Y.; Lee, N.-E. Stretchable, Transparent, Ultrasensitive, and Patchable Strain Sensor for Human-Machine Interfaces Comprising a Nanohybrid of Carbon Nanotubes and Conductive Elastomers. *ACS Nano* **2015**, *9*, 6252−6261.
(19) Choi, T. Y.; Hwang, B.-U.; Kim, B.-Y.; Trung, T. Q.; Nam, Y. H.; Kim, D.-N.; Eom, K.; Lee, N.-E. Stretchable, Transparent, and Stretch-Unresponsive Capacitive Touch Sensor Array with Selectively Patterned Silver Nanowires/Reduced Graphene Oxide Electrodes. *ACS Appl. Mater. Interfaces* **2017**, *9*, 18022−18030.
(20) Ho, D. H.; Sun, Q.; Kim, S. Y.; Han, J. T.; Kim, D. H.; Cho, J. H. Stretchable and Multimodal All Graphene Electronic Skin. *Adv. Mater.* **2016**, *28*, 2601−2608.
(21) Lipomi, D. J.; Vosgueritchian, M.; Tee, B. C.-K.; Hellstrom, S. L.; Lee, J. A.; Fox, C. H.; Bao, Z. Skin-like Pressure and Strain Sensors Based on Transparent Elastic Films of Carbon Nanotubes. *Nat. Nanotechnol.* **2011**, *6*, 788−792.

DOI: 10.1021/acsami.9b02049
ACS Appl. Mater. Interfaces 2019, 11, 14997−15006

(22) Chen, S.; Wu, N.; Ma, L.; Lin, S.; Yuan, F.; Xu, Z.; Li, W.; Wang, B.; Zhou, J. Noncontact Heartbeat and Respiration Monitoring Based on a Hollow Microstructured Self-Powered Pressure Sensor. *ACS Appl. Mater. Interfaces* **2018**, *10*, 3660−3667.
(23) Wang, S.; Xie, Y.; Niu, S.; Lin, L.; Wang, Z. L. Freestanding Triboelectric-Layer-Based Nanogenerators for Harvesting Energy from a Moving Object or Human Motion in Contact and Non-contact Modes. *Adv. Mater.* **2014**, *26*, 2818−2824.
(24) Hammock, M. L.; Chortos, A.; Tee, B. C.-K.; Tok, J. B.-H.; Bao, Z. 25th Anniversary Article: The Evolution of Electronic Skin (E-Skin): A Brief History, Design Considerations, and Recent Progress. *Adv. Mater.* **2013**, *25*, 5997−6038.
(25) Tee, B. C.-K.; Chortos, A.; Dunn, R. R.; Schwartz, G.; Eason, E.; Bao, Z. Tunable Flexible Pressure Sensors using Microstructured Elastomer Geometries for Intuitive Electronics. *Adv. Funct. Mater.* **2015**, *24*, 5427−5434.
(26) Mannsfeld, S. C. B.; Tee, B. C.-K.; Stoltenberg, R. M.; Chen, C. V. H.-H.; Barman, S.; Muir, B. V. O.; Sokolov, A. N.; Reese, C.; Bao, Z. Highly Sensitive Flexible Pressure Sensors with Microstructured Rubber Dielectric Layers. *Nat. Mater.* **2010**, *9*, 859−864.
(27) Cheng, W.; Wang, J.; Ma, Z.; Yan, K.; Wang, Y.; Wang, H.; Li, S.; Li, Y.; Pan, L.; Shi, Y. Flexible Pressure Sensor with High Sensitivity and Low Hysteresis based on a Hierarchically Micro-structured Electrode. *IEEE Electron Device Lett.* **2018**, *39*, 288−291.
(28) Cho, S. H.; Lee, S. W.; Yu, S.; Kim, H.; Chang, S.; Kang, D.; Hwang, I.; Kang, H. S.; Jeong, B.; Kim, E. H.; Cho, K. L.; Lee, H.; Shim, W.; Park, C. Pyramidal Ionic Gels for Sensing Broad-Range Pressures with High Sensitivity. *ACS Appl. Mater. Interfaces* **2017**, *9*, 10128−10135.
(29) Qiu, Z.; Wan, Y.; Zhou, W.; Yang, J.; Yang, J.; Huang, J.; Zhang, J.; Liu, Q.; Huang, S.; Bai, N.; Wu, W.; Wang, H.; Guo, C. F. Skin with Biomimetic Dielectric Layer Templated from Calathea Zebrine Leaf. *Adv. Funct. Mater.* **2018**, *28*, 1802343.
(30) Jang, S.; Jee, E.; Choi, D.; Kim, W.; Kim, J. S.; Amoli, V.; Sung, T.; Choi, D.; Kim, D. H.; Kwon, J.-Y. Ultrasensitive, Low-Power Oxide Transistor-Based Mechanotransducer with Microstructured, Deformable Ionic Dielectrics. *ACS Appl. Mater. Interfaces* **2018**, *10*, 31472−31479.
(31) Shuai, X.; Zhu, P.; Zeng, W.; Hu, Y.; Liang, X.; Zhang, Y.; Sun, R.; Wong, C.-p. Highly Sensitive Flexible Pressure Sensor Based on Silver Nanowires-Embedded Polydimethylsiloxane Electrode with Microarray Structure. *ACS Appl. Mater. Interfaces* **2017**, *9*, 26314−26324.
(32) Joo, Y.; Yoon, J.; Ha, J.; Kim, T.; Lee, S.; Lee, B.; Pang, C.; Hong, Y. Highly Sensitive and Bendable Capacitive Pressure Sensor and Its Application to 1 V Operation Pressure-Sensitive Transistor. *Adv. Electrode Mater.* **2017**, *3*, 1600455.
(33) Joo, Y.; Byun, J.; Seong, N.; Ha, J.; Kim, H.; Kim, S.; Kim, T.; Im, H.; Kim, D.; Hong, Y. Silver Nanowire-embedded PDMS with A Multiscale Structure for A Highly Sensitive and Robust Flexible Pressure Sensor. *Nanoscale* **2015**, *7*, 6208−6215.
(34) Lee, K.; Lee, J.; Kim, G.; Kim, Y.; Kang, S.; Cho, S.; Kim, S.; Kim, J.-K.; Lee, W.; Kim, D.-E.; Kang, D.; Lee, T.; Shim, W. Rough-Surface-Enabled Capacitive Pressure Sensors with 3D Touch Capability. *Small* **2017**, *13*, 1700368.
(35) Wan, Y.; Qiu, Z.; Hong, Y.; Wang, Y.; Zhang, J.; Liu, Q.; Wu, Z.; Guo, C. F. A Highly Sensitive Flexible Capacitive Tactile Sensor with Sparse and High-Aspect-Ratio Microstructures. *Adv. Electrode Mater.* **2018**, *4*, 1700586.
(36) Luo, S.; Yang, J.; Song, X.; Zhou, X.; Yu, L.; Sun, T.; Yu, C.; Huang, D.; Du, C.; Wei, D. Tunable-Sensitivity Flexible Pressure Sensor based on Graphene Transparent Electrode. *Solid-State Electron.* **2018**, *145*, 29−33.
(37) Liang, X.; Sperling, B. A.; Calizo, I.; Cheng, G.; Hacker, C. A.; Zhang, Q.; Obeng, Y.; Yan, K.; Peng, H.; Li, Q.; Zhu, H.; Hight Walker, A. R.; Liu, Z.; Peng, L.-m.; Richter, C. A. Clean and Crackless Transfer of Graphene. *ACS Nano* **2011**, *5*, 9144−9153.
(38) Kang, J.; Shin, D.; Bae, S.; Hong, B. H. Graphene transfer: key for applications. *Nanoscale* **2012**, *4*, 5527−5537.
(39) Yang, J.; Liu, P.; Wei, X.; Luo, W.; Yang, J.; Jiang, H.; Wei, D.; Shi, R.; Shi, H. Surface Engineering of Graphene Composite Transparent Electrodes for High-Performance Flexible Triboelectric Nanogenerators and Self-Powered Sensors. *ACS Appl. Mater. Interfaces* **2017**, *9*, 36017−36025.
(40) Goli, P.; Ning, H.; Li, X.; Lu, C. Y.; Novoselov, K. S.; Balandin, A. A. Thermal Properties of Graphene-Copper-Graphene Heterogeneous Films. *Nano Lett.* **2014**, *14*, 1497−1503.
(41) Song, X.; Yang, J.; Ran, Q.; Wei, D.; Fang, L.; Shi, H.; Du, C. 3-D Conformal Graphene for Stretchable and Bendable Transparent Conductive Film. *J. Mater. Chem. C* **2015**, *3*, 12379−12384.
(42) Bae, G. Y.; Pak, S. W.; Kim, D.; Lee, G.; Kim, D. H.; Chung, Y.; Cho, K. Linearly and Highly Pressure-Sensitive Electronic Skin Based on a Bioinspired Hierarchical Structural Array. *Adv. Mater.* **2016**, *28*, 5300−5306.
(43) Ferrari, A. C.; Meyer, J. C.; Scardaci, V.; Casiraghi, C.; Lazzeri, M.; Mauri, F.; Piscanec, S.; Jiang, D.; Novoselov, K. S.; Roth, S.; Geim, A. K. Raman Spectrum of Graphene and Graphene Layers. *Phys. Rev. Lett.* **2006**, *97*, 187401.
(44) Chortos, A.; Bao, Z. Skin-inspired electronic devices. *Mater. Today* **2014**, *17*, 321−331.
(45) Nichols, W. Clinical Measurement of Arterial Stiffness Obtained from Noninvasive Pressure Waveforms. *Am. J. Hypertens.* **2005**, *18*, 3−10.
(46) Fu, X.; Dong, H.; Zhen, Y.; Hu, W. Solution-Processed Large-Area Nanocrystal Arrays of Metal-Organic Frameworks as Wearable, Ultrasensitive, Electronic Skin for Health Monitoring. *Small* **2015**, *11*, 3351−3356.
(47) Boutry, C. M.; Negre, M.; Jorda, M.; Vardoulis, O.; Chortos, A.; Khatib, O.; Bao, Z. A Hierarchically Patterned, Bioinspired E-skin Able to Detect the Direction of Applied Pressure for Robotics. *Sci. Rob.* **2018**, *3*, No. eaau6914.

DOI: 10.1021/acsami.9b02049
ACS Appl. Mater. Interfaces 2019, 11, 14997−15006